THEORETICAL AND EXPERIMENTAL ANALYSIS OF THE BEARING JOURNAL MOTION DUE TO FLUID FORCE CAUSED BY THE OIL FILM

[1]Technical University of Ostrava, Faculty of Mech. Engineering Department of Control Systems and Instrumentation, Ostrava, Czech Republic

[2] Technical University of Ostrava, Faculty of Mech. Engineering, Department of Hydraulics, Ostrava, Czech Republic

[3] TECHLAB Ltd., Prague, Czech Republic

e-mail : jiri.tuma@vsb.cz

The paper relates to the fluid force acting on the journal of the slide bearings and its movement at stable lubrication. These forces can be calculated using the Reynolds equation. The analysis is based on the solution of the simplified equation and the experimental verification with the use of the test rig. The assumptions are verified by the numerical solution of the Reynolds equation by the FVM method.

KEYWORDS

journal bearings, Reynolds equation, fluid forces, Muszynska model

1 INTRODUCTION

An analysis of the behaviour of active vibration control systems requires describing a controlled system with the use of the linear equations that are suitable for the calculation of the system transfer functions and the controller adjustment [Tůma 2017]. For this purpose, there is a sufficient model designed by Muszynska [Muszynska 1986] because it allows deriving linear transmission functions that are useful for analyzing the control circuit and calculating the bearing radial stiffness. The disadvantage of this model is that the parameters of the Muszynska model cannot be calculated from bearing dimensions and lubricant properties. This analysis, however, is aimed at the calculation of the stiffness and damping matrices of the motion equation with the use of the Reynolds equation to estimate the behaviour of the journal bearing at the extra high rotational speed. Instead of numerical integration of the Reynolds equation, the derivation of the formulas to calculate the model parameters is used. For verification of the numerical solutions of the full three-dimensional fluid flow model (Navier Stokes equations) using finite volume method is applied.

2 INSTRUMENTATIONS

As has been said, we are interested in high-speed hydrodynamic journal bearings. We have a test rig with a rotor on two sliding bearings with these parameters: The span of bearing pedestals is of 200 mm, the journal diameter is of 30 mm, the radial clearance is of 60 µm, and the length-to-diameter ratio is equal to about 0.77. The rotor drives an induction motor that is powered by a frequency converter up to 400 Hz so that maximum speed can be up to 23,000 RPM. A sketch of the test rig is shown in Fig. 1.
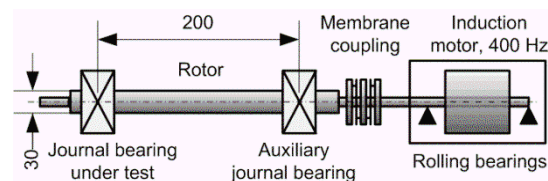
Figure 1. Sketch of the test rig

The test rig was completed for tests of actively controlled bearings with the use of piezoactuators. However, this article focuses only on the function of conventional sliding bearings, namely the movement of the bearing journal in the bushing. For the experimentation, proximity sensors and a rotational speed sensor are the most important. The installation of the sensors is shown in Fig. 2. During the tests, the oil temperature at the bearing outlet can be recorded. The oil pressure at the output of the oil pump is checked by a pressure gauge. Run-up and coast-down can take up to two minutes, and therefore these variables do not change.

Figure 2. Proximity sensors and a rotational speed sensor

The position of the journal is measured by a pair of the proximity probes which are capacitive sensors originated from the Micro-epsilon Company. The sensors are of the capaNCDT CS05 type with a measurement range of 0.5 mm. Measurement error is less than 1 micrometer. An advantage of the capacitive sensors is that it is not necessary to ground the shaft. Previously, we used the sensors based on the eddy current principle. The error of these sensors was ten times greater than that of the capacitance sensors, which is unacceptable for measuring the movements of the bearing journal in the range of +/- 60 micrometers. The position of the bearing journal is filtered by the Kalman filter. The covariance of the measurement error corresponds to the sensor error. The filter setting is the same as [Welch 1997].

The rotor rotational speed is evaluated from a tacho-signal in the form of the pulse string. The pulses are generated by the laser sensor originated at the BK Company. It is of the VLS Series (Optical Speed Sensor) type with the measurement range up to 250,000 RPM.

3 EXPERIMENTS

Special oil for high-speed spindle bearing of the OL-P03 type was used for testing (VG 10 grade, viscosity μ=0.027 Pa.s @ 20°C). Tests were carried out without preheating the lubricant at a normal temperature. The journal bearing cross-section is shown in Fig. 3.
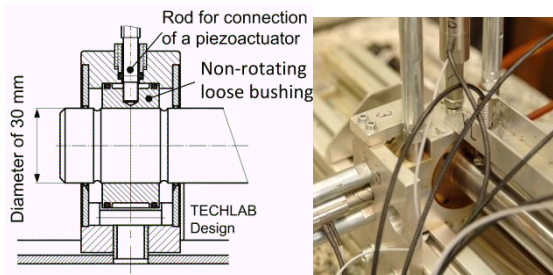
Figure 3. Side view technical drawing and a photo of bearing housing

The operating conditions of the hydrodynamic bearing are described by the Sommerfeld number [Budynas 2011]

$$S = (R/c)^2 \, \mu N/P, \qquad (1)$$

where N is a rotational speed of the rotor in rev/s, μ is a dynamic viscosity in Pa.s, R is a radius of the journal, c is a radial clearance, P is a load per unit of projected bearing area ($2RL$) in N/m², where L is a bearing length.

The value of the Sommerfeld number for the given bearing size and the rotor mass of 0.83 kg is as follows $S = 0.014 \times N$, where N is the mentioned rotational speed.

The magnitude of friction coefficient in the plain bearings was analyzed in the past by the McKee brothers [McKee 1932]. It has been found that bearing friction is dependent on a dimensionless bearing characteristic given by a ratio $\mu N/P$ whose parameters are defined above. If the rotor does not rotate or rotate slowly, there is only a very thin-film between the journal and the bushing. Boundary, or thin-film, unstable lubrication occurs with a considerably increased coefficient of friction. Many experiments show that the journal axis moves chaotically at low speeds or the journal starts to oscillate. It is uncertain at the start of run-up whether the axle of the bearing journal moves to the left or right, regardless of the direction of rotation. Only when the specified speed limit is exceeded the lubrication becomes stable, and thick-film of the lubricant is formed and the trajectory of motion can be predicted. The limit value of the bearing characteristic for the boundary lubrication is described in [Budynas 2011]. Designers keep value $\mu N/P \geq 1.7 \times 10^{-6}$ (reyn x rev/s/psi), which is about five times the value the McKee brothers have determined. The measurement in our test rig shows the limit of the unstable lubrication at about 1,000 RPM, which corresponds to the value of the dimensionless characteristic $\mu N/P$ equaled to 3.8×10^{-5} (Pa.s x rev/s/Pa) when using SI units for the input parameters. Our estimate for the lower limit of stable lubrication corresponds to the recommendations in the handbook [Budynas 2011]. In experiments with the active vibration control, the feedback is closed only for stable lubrication.
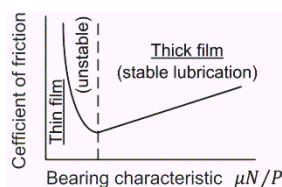
Figure 4. Journal bearing friction in the region of thin film lubrication [Budynas 2011]

The coefficient of friction decreases from a considerable initial value. Exceeding the speed limit leads to stable lubrication with a low coefficient of friction because the changes are self-correcting. By the viscous friction theory, the coefficient of friction is proportional to the speed of rotation as is shown in Fig. 4.

An example of a gradual change of position of the bearing journal centre during an increase in speed up to 7,000 RPM at the constant increase rate is shown in Fig. 5. The lubrication is unstable in the range up to about 1,200 RPM and is accompanied by oscillations.

The reason for the oscillations is the step change of speed to about 300 RPM after switching on because it is not possible to increase the rotational speed continuously from zero. Hydrodynamic stable lubrication at stable motion is produced for rotational speed up to 5,000 RPM. Motion instability of the whirl type occurs when this speed of 5,000 RPM is exceeded. Fluid force makes sense to be modeled just for stable motion and lubrication. It is almost impossible to determine the initial conditions for unstable lubrication.
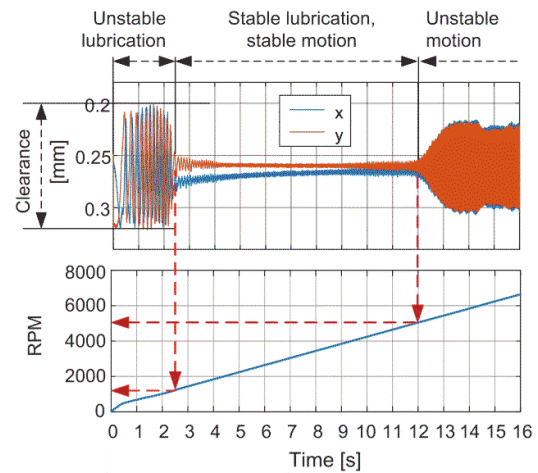
Figure 5. The run-up of a journal bearing

Notice that the centre of the journal rises to the level of the centre of the bearing bore and gradually approaches this centre so that the small eccentricity gradually decreases to zero as is shown on the right panel of Fig. 6. The data for this orbit was approximated by the 5-degree polynomial in the time interval which begins at the 3rd second and ends at the 12th second. The difference between thin and thick film lubrication is also evident on the left panel of Fig. 6, which depicts an orbit plot for the entire measurement time up to 16th second.
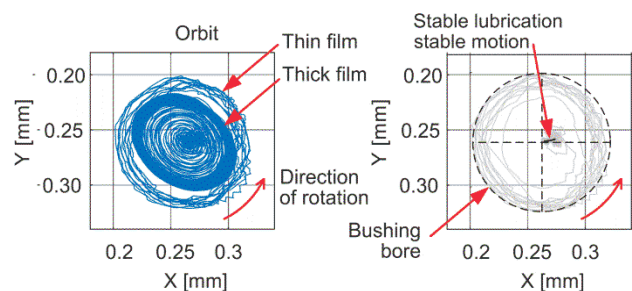
Figure 6. Orbit plot corresponding to data from Figure 5 (radial clearance 60 µm)

4 MATHEMATICAL MODEL

4.1 Equation of motion

The bearing journal can be considered as a rigid body rotating within the bearing housing at an angular velocity Ω. For simplicity, it is assumed that the rotation axis does not change its direction in contrast to [Wagnerova 2016]. Fluid forces are caused by the hydrodynamic pressure generated in the oil film,

whose total mass relative to the journal and rotor is negligible. The oil pumped by the rotating journal surface produces an oil wedge that lifts up the bearing journal so that it does not touch the inner walls of the housing. The coordinate system of a cylindrical journal bearing is shown on the left side in Fig. 7. The planar motion of the bearing journal at the x and y coordinates can be described by two motion equations arranged into a matrix equation

$$\begin{bmatrix} M & 0 \\ 0 & M \end{bmatrix}\begin{bmatrix} \ddot{x} \\ \ddot{y} \end{bmatrix} + \begin{bmatrix} B_{XX} & B_{XY} \\ B_{YX} & B_{YY} \end{bmatrix}\begin{bmatrix} \dot{x} \\ \dot{y} \end{bmatrix} + \begin{bmatrix} C_{XX} & C_{XY} \\ C_{YX} & C_{YY} \end{bmatrix}\begin{bmatrix} x \\ y \end{bmatrix} = \begin{bmatrix} F_X \\ F_Y \end{bmatrix}, \quad (2)$$

where M is a mass of the rotor, F_X is a force acting on the journal in the horizontal direction, F_Y is a force acting on the journal in the vertical direction, C_{UV} is a stiffness coefficient, B_{UV} is a damping coefficient, where U is equal to X or Y and V is equal to X or Y as well.

In addition to force components in the horizontal and vertical directions, the force balance will be solved in other possible directions. Force in the direction of the line of the centers is denoted as a direct force F_D while force which is perpendicular to the line of centers is denoted as a quadrature force F_Q. Both these forces balance the gravity force G as is shown in the right panel of Fig. 7.

The system is described by two motion equations, and therefore the total order of the system is four. This system may become unstable even for positive parameter values such as stiffness and damping.
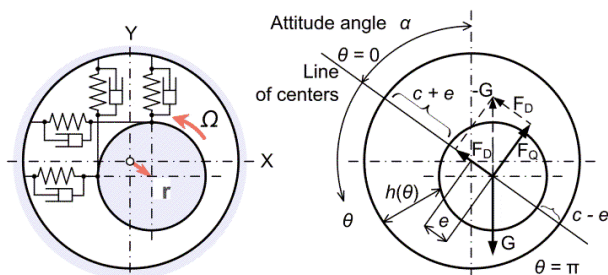
Figure 7. A cross-section of the hydrodynamic bearing

4.2 Muszynska model

The motion equation of the rotor with the journal bearing in coordinates x and y was designed by Muszynska. The derivation is based on the design of the formula to calculate the already mentioned direct and quadrature forces. Compared to Eq. (2), the stiffness and damping matrices are designed in such a way that the oil film is replaced by a spring and a dashpot system that rotates at an angular velocity Ω, where λ is a dimensionless parameter, which is slightly less than 0.5. The stiffness of the spring is designated by K and the damper has a damping factor D

$$\begin{bmatrix} M & 0 \\ 0 & M \end{bmatrix}\begin{bmatrix} \ddot{x} \\ \ddot{y} \end{bmatrix} + \begin{bmatrix} D & 0 \\ 0 & D \end{bmatrix}\begin{bmatrix} \dot{x} \\ \dot{y} \end{bmatrix} + \begin{bmatrix} K & D\lambda\Omega \\ -D\lambda\Omega & K \end{bmatrix}\begin{bmatrix} x \\ y \end{bmatrix} = \begin{bmatrix} F_X \\ F_Y \end{bmatrix}. \quad (3)$$

The derivation of the motion equation is described, for example, in [Tůma 2013]. No analytical way to calculate the value of unknown model parameters has been proposed. These parameters can be estimated only from a comparison of measurement and simulation.

4.3 Analytical solution of the Reynolds equation

The theory of hydrodynamic bearing is based on a differential equation derived by Osborne Reynolds. Reynolds equation is based on the following assumptions: The lubricant obeys Newton's law of viscosity and is incompressible. The inertia forces of the oil film are negligible. The viscosity μ of the lubricant is constant, and there is a continuous supply of lubricant. The effect of the curvature of the film concerning film thickness is neglected. It is assumed that the film is so thin that the pressure is constant across the film thickness. The shaft and bearing are rigid.

Furthermore, it is assumed that the thickness h of the oil film depends on the other two coordinates, namely the coordinate z along the axis of rotation and the location on the perimeter of the journal which is described by the angle θ as is shown on the right side in Fig. 7. If the radius of the bearing journal is equal to R, then the most general version of the Reynolds equation for calculation the of the oil pressure distribution $p(\theta, z)$ is as follows [Dwivedy 2006]

$$\frac{1}{R^2}\frac{\partial}{\partial \theta}\left(h^3\frac{\partial p}{\partial \theta}\right) + \frac{\partial}{\partial z}\left(h^3\frac{\partial p}{\partial z}\right) = 6\mu\Omega\frac{\partial h}{\partial \theta} + 12\mu\frac{\partial h}{\partial t}. \quad (4)$$

There is no analytical solution for the Reynolds equation.

During operation, the journal axis shifts from the centre of the bearing bushing to the distance of e, called eccentricity, which is related to a radial clearance c. Variable is called an eccentricity ratio $n = e/c$. The film thickness as a function of θ is defined as follows

$$h = c(1 + n\cos\theta). \quad (5)$$

The oil film moves in adjacent parallel layers at different speeds, and shear stress results between them. The oil layer at the surface of the journal moves at the peripheral velocity of the journal while the oil layers at the surface of the bearing bushing don't move (at zero velocity). The surface of the journal moves at a velocity of $U = R\Omega$ in m/s. Reynolds equation will be solved for the steady-state and independence of the pressure distribution on the coordinate of z

$$\frac{d}{d\theta}\left[h^3\frac{dp}{d\theta}\right] = 6\mu UR\frac{dh}{d\theta}. \quad (6)$$

On double integrating, see [Dwivedy 2006], we get

$$h^3\frac{dp}{d\theta} = 6\mu UR\int\frac{dh}{d\theta}d\theta = 6\mu URh + K$$
$$\frac{dp}{d\theta} = 6\mu UR\left[\frac{1}{(1+n\cos\theta)^2} + \frac{K_1}{c(1+n\cos\theta)^3}\right]$$
$$p(\theta) = \frac{6\mu UR}{c^2}\int\left[\frac{d\theta}{(1+n\cos\theta)^2} + \frac{K_1 d\theta}{c(1+n\cos\theta)^3}\right] + p_0, \quad (7)$$

where K, K_1, and p_0 are integration constants.

The solution must meet the boundary condition

$$p(\theta = 0) = p(\theta = 2\pi) \Rightarrow p(\theta = 0) - p(\theta = 2\pi) = 0, \quad (8)$$

which gives

$$\frac{6\mu UR}{c^2}\int_{\theta=0}^{\theta=2\pi}\left[\frac{1}{(1+n\cos\theta)^2}+\frac{K_1}{c(1+n\cos\theta)^3}\right]d\theta=0$$
$$\Rightarrow \frac{K_1}{c}=-\frac{\int_{\theta=0}^{\theta=2\pi}1/((1+n\cos\theta)^2)d\theta}{\int_{\theta=0}^{\theta=2\pi}1/(c(1+n\cos\theta)^3)d\theta}$$
(9)

On simplifying, we get a formula for calculating the first integration constant K_1

$$K_1=2c(n^2-1)/(n^2+2).$$ (10)

Extreme oil pressure values as a function of the attitude angle θ are achieved if $dp/d\theta=0$.

$$K_1=-h=-c(1+n\cos\theta)$$
(11)

The first integration constant is related to the thickness of the oil film at the perimeter of the journal, where the maximum and minimum oil pressure is achieved

$$h_m=(h)_{p=min}=(h)_{p=max}=-K_1=\frac{2c(1-n^2)}{(n^2+2)}$$ (12)

The attitude angle where the maximum and minimum pressure occur is given by

$$\cos\theta_m=-3n/(n^2+2)$$ (13)

The result of double integration is as follows

$$p(\theta)=\frac{6\mu UR}{c^2}\frac{n(2+n\cos\theta)\sin\theta}{(n^2+2)(1+n\cos\theta)^2}+p_0=\frac{6\mu UR}{c^2}\beta(n,\theta)+p_0.$$ (14)

The first integration constant was selected to meet the boundary condition $p_0(0)=p_0(2\pi)$ as is described by Dwivedi et al.. The oil pressure distribution on the journal for $n=0,0.1,0.2,\cdots,0.9$ is shown in Fig. 8. It should be noticed that the second integration constant has not any effect on the force excited by the oil pressure. The sub atmospheric pressure creates a condition for the formation of the cavitation zones.
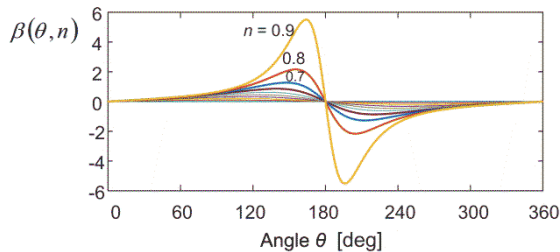
Figure 8. Pressure distribution along the angular coordinate θ

4.4 Fluid force

The forces acting on the journal in the centre of gravity along the bearing length of L can be calculated for the direction of the line of the centres and the perpendicular direction. Force in the direction of the line of centres is denoted as a direct force F_D while force which is perpendicular to the line of centers is denoted as a quadrature force F_Q. Both these forces balance the gravity force G as is shown in Fig. 7

$$F_D=\int_0^{2\pi}p_\theta\cos(\pi-\theta)LR\,d\theta=$$
$$=F_N\int_0^{2\pi}\beta(\theta,n)\cos(\pi-\theta)\,d\theta=F_N\beta_D(n)$$
$$F_Q=\int_0^{2\pi}p_\theta\sin(\pi-\theta)LR\,d\theta=$$
$$=F_N\int_0^{2\pi}\beta(\theta,n)\sin(\pi-\theta)\,d\theta=F_N\beta_Q(n)$$
(15)

where the force F_N can be designated as a nominal force because it corresponds to the maximum force according to the linear model ($n=1$)

$$F_N=6\mu UR^2L/c^2.$$ (16)

Note that according to formula (14) the pressure on the part of the journal surface is negative, which is, in fact, a relative negative pressure. Since the pressure distribution is anti-symmetric with respect to $\theta=\pi$, without evidence, it is clear that these formulas can be applied. Only quadrature force $F_Q>0$ acts on the bearing journal and the direct force are zero $F_D=0$, as is shown on the upper panel in Fig. 9.

The nominal force that multiplies the dimensionless functions $\beta_D(n)$ and $\beta_Q(n)$ can be calculated with the use of the dimensionless Sommerfeld number S and the load P per unit of projected bearing area as follows

$$F_N=6\mu UR^2L/c^2=6\pi SG,$$ (17)

where G is a gravity force.

For speeds ranging from 1,250 to 5,000 RPM, the force factor F_N varies from 0.46 to 1.8 kN. However, this force is reduced by multiplying the coefficients $\beta_D(n)$ and $\beta_Q(n)$ which depend on the eccentricity ratio n ranging from 0 to 0.33 (0.02/0.06). This case can only theoretically arise in an entirely flooded plain bearing with a vertical axis. The balance of forces F_D, F_Q, and F_Q allows to calculate an attitude angle α, see the bottom panel in Fig. 10 which is a part of the next subchapter

$$\alpha=\arctan(\beta_D(n)/\beta_Q(n))$$ (18)
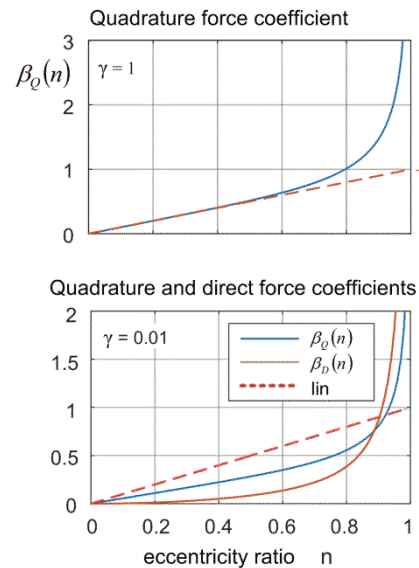
Figure 9. Dependence of the direct and quadrature force on the eccentricity ratio

The presence of direct force can be explained, e.g. by the cavitation or the inability to achieve high vacuum, but the mathematical model is more complicated [Ferfecki 2012]. The lubricant flows through the bearing, but in the part of the bearing journal circumference where the pressure is below the barometric pressure, the lubricant can also be sucked. The magnitude of the negative pressure for $\pi < \theta < 2\pi$ is multiplied by a factor γ. Therefore the total force is given by the sum of integrals (15) as follows

$$\begin{bmatrix} F_D \\ F_Q \end{bmatrix} = \int_0^{\pi} (\dots)\mathrm{d}\theta + \gamma \int_{\pi}^{2\pi} (\dots)\mathrm{d}\theta, \tag{19}$$

The effect of negative pressure reduction is demonstrated in the bottom panel of Fig. 9. Negative pressure is limited to 1% of the magnitude of positive pressure for the angle interval of $0 < \theta < \pi$. The formulas for the calculation of the quadrature and direct forces contain the same factor $F_N = 6\mu U R^2 L/c^2$ and hence the dependence on the peripheral speed U and therefore on the rotor angular velocity. The coefficients $\beta_Q(n)$ and $\beta_D(n)$ differ considerably. In the experiment, the results of which are shown in Fig. 5, the eccentricity ratio decreases approximately from 0.3 to 0.07 in the operation at the stable bearing position and stable lubrication. The diagrams confirm the linearity of the quadrature and direct force to eccentricity ratio up to 0.6. The $\beta_Q(n)$ and $\beta_D(n)$ coefficients can be approximated in this range as a linear function

$$\begin{aligned} \beta_Q(n) &\approx qcn = qe \\ \beta_D(n) &\approx dcn = de, \end{aligned} \tag{20}$$

where q determines the quadrature stiffness $C_Q = 6\mu U R^2 L/c^2 \times q$ and d determines the direct stiffness $C_D = 6\mu U R^2 L/c^2 \times d$.
The stiffness in the directions of the Cartesian coordinates x, y, and the attitude angle α which is defined in Fig. 5 can be obtained by substitution

$$\begin{aligned} x(t) &= -e \sin \alpha \\ y(t) &= +e \cos \alpha. \end{aligned} \tag{21}$$

The vector of the direct and quadrature forces depends on the coordinates x, y according to the following formula

$$\begin{bmatrix} -C_D e \sin \alpha + C_Q e \cos \alpha \\ C_Q e \sin \alpha + C_D e \cos \alpha \end{bmatrix} = \begin{bmatrix} C_D x + C_Q y \\ -C_Q x + C_D y \end{bmatrix} = \\ = \begin{bmatrix} C_D & C_Q \\ -C_Q & C_D \end{bmatrix} \begin{bmatrix} x \\ y \end{bmatrix}. \tag{22}$$

The cross-coupled stiffness $D\lambda\Omega$ according to the Muszynska model corresponds to the expression $6\mu U R^2 L/c^2 \times q$. The direct stiffness K is orderly less than the cross-coupled stiffness; however, the analytical calculation of the stiffness matrix shows the dependence on the rotational speed.

The damping matrix can be derived based on its relationship to the stiffness matrix according to the model that was designed by Muszynska.

$$\begin{bmatrix} D & 0 \\ 0 & D \end{bmatrix} \begin{bmatrix} \dot{x} \\ \dot{y} \end{bmatrix} = \begin{bmatrix} C_Q/\lambda\Omega & 0 \\ 0 & C_Q/\lambda\Omega \end{bmatrix} \begin{bmatrix} \dot{x} \\ \dot{y} \end{bmatrix}. \tag{23}$$

As is $D = C_Q/\lambda\Omega$ the damping coefficient D is a constant. The motion equation for the rigid rotor in the plain bearing is as follows

$$\begin{bmatrix} M & 0 \\ 0 & M \end{bmatrix} \begin{bmatrix} \ddot{x} \\ \ddot{y} \end{bmatrix} + \begin{bmatrix} C_Q/\lambda\Omega & 0 \\ 0 & C_Q/\lambda\Omega \end{bmatrix} \begin{bmatrix} \dot{x} \\ \dot{y} \end{bmatrix} + \begin{bmatrix} C_D & C_Q \\ -C_Q & C_D \end{bmatrix} \begin{bmatrix} x \\ y \end{bmatrix} = \begin{bmatrix} F_X \\ F_Y \end{bmatrix}. \tag{24}$$

The sum of direct and quadrature forces must compensate for the gravitational force that does not depend on the speed of rotation. The suitability of this model is confirmed by [Mendes 2014].

4.5 Force balance

As shown in Fig. 7, three static forces acting on the bearing journal, namely direct force F_D, quadrature force F_Q, and gravitational force G. The following equation is a condition of equilibrium of these forces

$$G^2 = F_D{}^2 + F_Q{}^2. \tag{25}$$

On substituting, we get

$$G^2 = F_N^2 \left(\left(\beta_D(n)\right)^2 + \left(\beta_Q(n)\right)^2 \right). \tag{26}$$

Continuing the equation editing leads to the formula

$$\left(\beta_D(n)\right)^2 + \left(\beta_Q(n)\right)^2 = 1/(6\pi S)^2. \tag{27}$$

The expression on the right side of the previous formula can be calculated from the Sommerfeld number S for a given rotation speed N, and the load P per unit of projected bearing area. Since both coefficients $\beta_Q(n)$ and $\beta_D(n)$ depend on the eccentricity ratio n, this unknown quantity can be determined just like the attitude angle α, see Fig. 10, and the journal centre coordinates as a function of the speed of rotation.
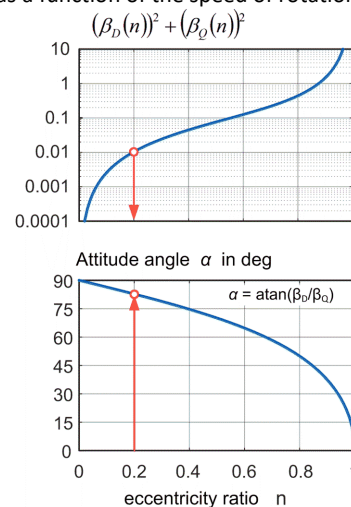
Figure 10. Calculation of the attitude angle α, and the journal centre coordinates

If the attitude angle approaches the angle of $\pi/2$ in the radians, then the gravitational force is balanced only by the quadrature force. This state represents the stability limit. The experiment described in this article demonstrates the fact that stable lubrication occurs when the eccentricity ratio n is decreased to below the value of 0.33 which happens after a certain speed margin has been exceeded. Unstable lubrication occurs during low revolutions when the eccentricity ratio is higher than the mentioned boundary. The problem of modelling the motion of the bearing journal at low rotational speeds raises the impossibility of determining the initial conditions.

5   NUMERICAL SOLUTION OF THE REYNOLDS EQUATION

The prerequisite for deriving a simplified fluid force calculation was the existence of cavitation or the inability to achieve the high vacuum due to the sucking out of lubricant from the outside of the bearing. This assumption has been verified by the numerical solution of the general Reynolds equation (4), including the assumption of the pressure compliance with barometric pressure at the edge of the bearing bushing. The calculation of the pressure distribution on the journal surface of the bearing of arbitrary length is based on the input data as the eccentricity e and a given speed in RPM. To obtain the realistic results, the actual eccentricity was deducted from the measurement in Fig. 5. Due to the rotational speed and flow velocity then the Reynolds number was determined for the flow in the gap, the value of which was meager. The flow was classified as laminar.

A significant result was the distribution of pressure on the bushing walls and the bearing journal as is shown in Fig. 11. Since the minimum pressure is approaching the vacuum pressure (zero absolute pressure), it seems that the oil flow does not show cavitation. The results of the simulation calculations confirm that the gravity force compensates for the quadrature force, which is many times larger than the direct force.

Simulation calculations were performed using the ANSYS-Fluent software, version 18.2.
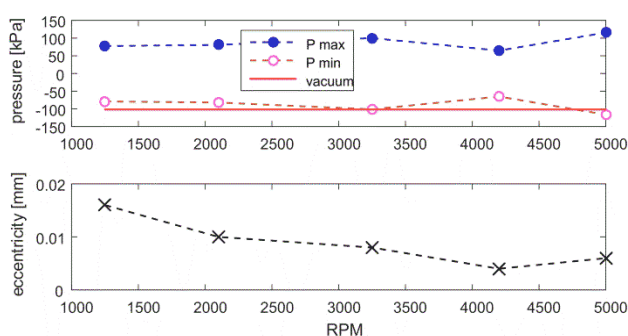
Figure 11. Dependence of max and min pressure on journal surface on speed and eccentricity

6   CONCLUSIONS

We recognize three operating modes for plain bearings. For low rotational speed, the lubrication is unstable, the lubrication and motion are stable at medium rotational speed, and for high rotational speed the motion is unstable and whirl or even whip vibrations are produced. This article focuses on a second operating mode where motion and lubrication are stable.
The key problem is the modeling of fluid force acting on the bearing journal. The calculation of the fluid force acting on the

bearing journal using the Reynolds equation shows that the stiffness matrix corresponds to the stiffness matrix according to the Muszynska model. This finding can only be applied for a rotational speed range where lubrication is stable, which is of course not at zero or low rotational speeds. From the Reynolds equation, unlike the Muszynska model, it follows that the elements on the main diagonal of the stiffness matrix are also dependent on the speed of rotation. The conclusions apply only to the range of magnitudes in which the formulas can be linearized. The numerical solution of the Reynolds equation confirms the possible occurrence of cavitations. The theoretical models are always unreliable and require comparative measurement on the test rig.

REFERENCES

[Budynas 2011] Budynas, R. G. and Nisbett, J. K. Shigley's mechanical engineering design, 9th edition. New York: McGraw-Hill, 2011. ISBN 978-0-07-352928-8.

[Dwivedy 2006] Dwivedy, S. K. and Tiwari, R. Dynamics of Machinery, A Lecture Notes, All India Council of Technical Education, March 2006.

[Ferfecki 2012] Ferfecki, P. and Zapomel, J. Investigation of vibration mitigation of flexible support rigid rotors equipped with controlled elements. In: 5th International Conference on Modeling of Mechanical and Mechatronic Systems, MMaMS 2012; Zemplinska Sirava; Slovakia, 6-8 November 2012, Vol- 48, (135-142).

[McKee 1932] McKee, S. A. and McKee, T. R. Journal Bearing Friction in the Region of Thin Film Lubrication, SAE J., vol. 31, 1932, pp. (T)371–377.

[Mendes 2014] Mendes, R. U. and Cavalca, K. J. On the Instability Threshold of Journal Bearing Supported Rotors. International Journal of Rotating Machinery. Vol. 2014, Article ID 351261.

[Muszynska 1986] Muszynska, A. Whirl and whip – rotor/bearing stability problems. Journal of Sound and Vibration. 1986, Vol. 110, Issue 3, (443-462).

[Tuma 2013] Tuma, J., Simek, J., Skuta, J. and Los, J. Active vibrations control of journal bearings with the use of piezoactuators. Mechanical Systems and Signal Processing, 2013, Vol. 36, (618-629).

[Tuma 2017] Tuma, J., Simek, J., Mahdal, M., Skuta, J. and Wagnerova, R. Actively Controlled Journal Bearings. In: H. Ecker, ed. Proc. 12th SIRM Conference, Graz, Österreich, 15. – 17., February 2017, (443-462).

[Wagnerova 2016] Wagnerova, R. and Tuma, J. Use of complex signals in modelling of journal bearings. In: 8th Vienna International Conference on Mathematical Modelling, MATHMOD 2015; Vienna; Austria; February 18-20 2015, (520-525).

[Welch 1997] Welch, D. and Bishop, G., An Introduction to the Kalman Filter, Dept of Computer Science University of North Carolina at Chapel Hill Chapel Hill, NC 27599-3175, September 17, 1997. <http://www.cs.unc.edu/~welch/kalman/>

CONTACTS:

Prof. Ing. Jiri Tuma, CSc. FEng.
Ing. Miroslav Pawlenka
Ing. Miroslav Mahdal, Ph.D.
VSB – Technical University of Ostrava
Faculty of Mech Engineering
Department of Control Systems andInstrumentation
17. listopadu 15, 708 33, Ostrava, Czech Republic
e-mail: jiri.tuma@vsb.cz
e-mail: miroslav.pawlenka@vsb.cz
e-mail: miroslav.mahdal@vsb.cz

Prof. RNDr. Milada Kozubkova, CSc.
VSB – Technical University of Ostrava
Faculty of Mech Engineering
Department of Hydraulics
17. listopadu 15, 708 33, Ostrava, Czech Republic
e-mail: milada.kozubkova@vsb.cz

Ing. Jiri Simek, CSc.
TECHLAB Ltd.
Sokolovska 207, 190 00, Praha 9, Czech Republic
e-mail: j.simek@techlab.cz